ISSN: 2277-3754
ISO 9001:2008 Certified
International Journal of Engineering and Innovative Technology (IJEIT)
Volume 4, Issue 3, September 2014

Contact Stress Analysis of Interference Fit Between V-band Clamp and Piping Systems

Zhengui Zhang, Peixuan Wu, Haiyan H Zhang

Abstract*—In this paper, a model of V-band clamp is built to determine the contact pressures generated between the piping systems, in particular, bellow and manifold. The approaches for this analysis include theoretical modeling, finite element analysis (FEA) using COMSOL multi-physicals, and experimental validations. Due to the spatial non-uniformities of the moment of inertia and section area of the clamp, the bending moment effect caused by offset of centroid lines between the trunnion and clamp is observed in simulation results. This effect leads to slight vertical displacement of the trunnion and high contact pressure beneath it. Given the geometry of the clamp and the piping systems, conformal and non-conformal contact analyses are discussed to present a more exact approximation of stress distribution beneath the trunnion. The analytical results are utilized to optimize the design of V-band clamp for releasing the peak stress beneath trunnion and eliminating its nearby warping effect.

***Index Terms*— Contact pressure, Interference fit, V-band clamp.**

I. INTRODUCTION

As an economical and reliable method, the V-band clamp connection is widely used for the piping systems and other tubing closures for decades in various environments, such as high temperature, and vibration conditions. However, the knowledge of the marman clamp systems from the testing data and the past experiences of both failures and successes were not well recorded, and its accumulation had little increment after it was first introduced. Even worse, its comprehensive documentation of the knowledge was rarely publicized. The theoretical analysis and the relevant research on the clamping system is greatly needed [1]. Reliable and persistent joint between rigid components receives more and more attention in industry, especially in the application of exhausted piping systems. In the case of V-band clamp, tangential tension induced by torque results in a radial force, and the corresponding axial load from wedging action of V-retainer works to seal the rigid components [2]. To reach reliable sealing, a tight and uniform interaction between the clamp and rigid components is expected, however, in reality, this kind of interaction is highly non-linear and affected by several factors, such as friction and load combinations [3]. Ideally, the distribution of circumferential force and contact pressure is exponential when friction is present [2]. In fact, the loading position and gap arrangement would affect the performance of the wedge effect, which causes the contact pressure to deviate from the ideal distribution. Node to node interaction model was employed to determine stress and displacement resulted from interference fit [4]. Mucha presented a shrink fit FEA simulation to give the radial stress at inner surface of the rings, and compare with the traditional Lame's equation[5]. The results indicated that stresses and deformation were different in the range of fit zone and highly affected by the geometry of the interference-fit two parts. Zhang proposed a more completed and accurate stress analysis than the traditional thick cylinder theory, which was utilized to refine the operations of the interference-fit assembly[6]. Oda studied the shrink fitted assembly with stress concentration on the contact surface, and manipulated the variable interference to obtain stress distribution uniformity[7]. However, the variable interference was meaningful in theoretical analysis, not yet feasible for the manufacturing process. Thus, specified geometric features must be considered in the theoretical analysis as guidance to predict the possible connection attributes of the clamp[8]. In order to meet the specific design requirements, the effect of the clamp parameters, such as V-segment number, size, and wedge angles, band, and T-bolt should be specified. This research is dedicated to investigate the distribution of the contact pressure of interference fit V-band clamp and piping systems and it can provide a proper solution to marmon system leakage which is a common problem in industries. FEA is employed to provide an economical, convenient and effective method in clamp jointing effect. A 3-D FEA model imported from Pro/E are established using COMSOL multi-physics to explore the near loading zone properties. A classical theoretical analysis combined with indirectly experiment measurement on the clamp's band is used to investigate the exponential distribution of contact pressure at those far away loading zone areas. With mechanical analysis based on the specific geometry of clamp, the abnormal distribution beneath and near the loading zone is explored.

II. THEORETICAL ANALYSIS AND EXPERIMENT RESULT

All components and nomenclatures of clamp are defined in Fig. 1(a). Radial force is induced during tightening of the trunnion nut. Fig. 1(b) shows the working principle of the interference fit clamp and piping systems, with the specified torque applied onto the nut and the band tightly clamped. Three contact pairs, i.e., manifold/clamp, clamp/bellow and manifold/bellow, provide the continuity of contact, with which the points of contact on both sides of the contact surface are assumed to have the same displacement. Lame's equation based on thick walled cylinders was applied usually to describe interference fit model in the elastic range. In that analysis, the contact pressure around the cylinders was assumed as constant, and the corresponding circumferential stress was in a liner relationship with the contact pressure.

ISSN: 2277-3754
ISO 9001:2008 Certified
International Journal of Engineering and Innovative Technology (IJEIT)
Volume 4, Issue 3, September 2014

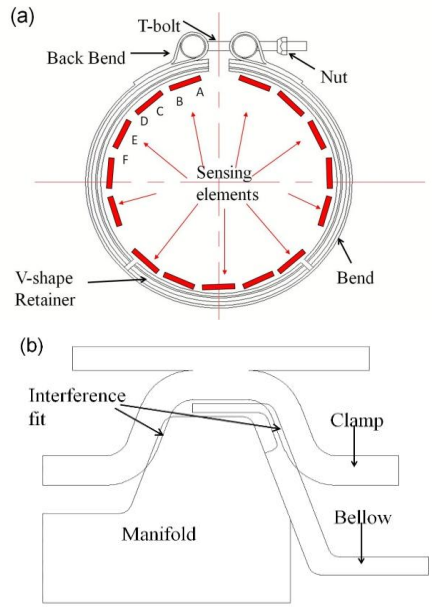

Fig 1. (a) Configuration of V-band clamp, (b) Interference fit assembly of clamp and piping systems

In industry, lubricant selection is important during assembly which greatly affects the final distribution of contact pressure. Shoghi[2] derived the static analysis with the consideration of friction effect on the V-band clamp, and derived the stress formulations of the initial bending stress σ_B, circumferential stress σ_α, contact pressure q, bending stress σ_b and longitudinal stress σ_L (see Table 1). In Table 1., y(m) is distance from the neutral axis; δ_H is horizontal displacement; ξ(rad) is the half angle of the top gap; θ(rad) is angle of any position; R(mm) is radius of clamp; β(rad) is angle of half clamp; F(N) is clamping load; μ is friction coefficient; ϕ(rad) is the V-section interval angle; t(mm) is thickness of V-shape retainer; A(m2) is the cross section area; q(N/m) is load in normal direction; p(N/m) is load in the radial direction; h(m) is the gap between clamp and flange; and f(m) is the thickness of flange edge.

Table 1. Static analysis with friction effect

Formulation
$\sigma_B = yE\delta_H(\cos\xi+\cos\theta)\Big/ R^2[\beta(\frac{1}{2}+\cos 2\beta)-\frac{3}{4}\sin 2\beta]$
$\sigma_\alpha = Fe^{\frac{-\mu(\beta-\theta)}{\sin\phi}} / A$
$q = p/2\sin\varphi = Fe^{\frac{-\mu(\beta-\theta)}{\sin\phi}} /(2R\sin\varphi)$
$\sigma_b = \frac{Mz}{I_1} = 3F_\beta(h\cos\phi + f\sin\phi)\exp[-\mu(\beta-\theta)/\sin\phi]\Big/ t^2 R\sin\phi$
$\sigma_L = F\exp[-\mu(\beta-\theta)/\sin\varphi]/2tR\tan\varphi$

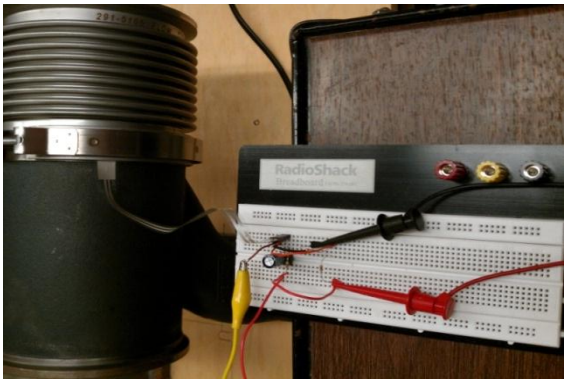

Fig 2. Piezoelectric sensor test platform with charge mode amplifier setup

An experiment is set up to verify the theoretical analysis on the circumferential stress and the contact pressure of the V-band clamp (Fig. 2). Piezoelectric sensor is a device that uses the piezoelectric effect to measure pressure, acceleration, strain or force by converting them to an electrical charge. The direct piezoelectric effect is that electrical polarization charges generate with an applied mechanical force on piezoelectric materials. In order to get radial load data of V-band clamp from piezoelectric sensors, necessary calibrations are made before the experiment. Ten PVDF (polymer polyvinylidene fluoride) piezoelectric sensors are evenly placed outside onto one side of the band to measure the circumferential strains. These sensors are not placed on the back bend and trunnion because of their different geometrical characteristics and RSW (resistance spot welding) spots. The 10th sensor is at the bottom of clamp and the 1st sensor is near the back bend of the clamp. With the data acquisition system, the voltage signals from the PVDF sensors are recorded. The measured results of the circumferential strain are plotted in Fig. 3(a). A peak stress at the 7th sensor location is observed. It is caused by the geometric change at the gap between the V-retainers. In Fig. 3(b), except the 7th sensor, the remaining data present the changing tendency of the circumferential strain. From the experiment results, it can be observed that the circumferential strain or force experiences a faster decline. Thus, it can be deduced that the contact pressure can decline in the same pattern and it can be calculated by multiplying the constant ratio 2Rsin (20^o)/A. The curve of calculated contact pressure is also plotted in Fig.3 (b) and the data is set in the range less than 1 in order to present the tendency of curve. In comparison with the experimental measurements, the theoretically estimated strain decreases slower along the clamp from the trunnion to the bottom of the clamp. The decline of the circumferential stress from the trunnion to the bottom is attributed to the friction effect, because the larger the friction effect is, the more the circumferential stress decreases. Therefore, a quick decrease of circumferential stress implies a higher friction and a higher contact pressure. Specifically, as shown in Fig.3 (b), significant deviations occur at the top and bottom of the clamp under torque 3Nm,

ISSN: 2277-3754
ISO 9001:2008 Certified
International Journal of Engineering and Innovative Technology (IJEIT)
Volume 4, Issue 3, September 2014

which implies that at the top and bottom of the clamp the high contact pressures present from the initial stage of installment.

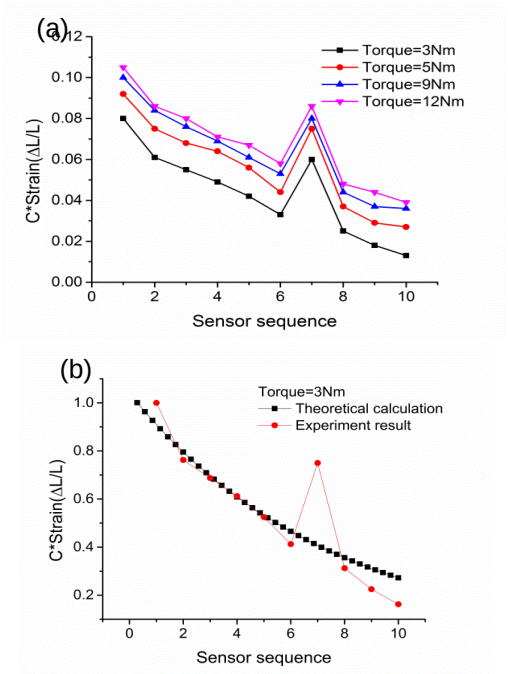

Fig 3. (a) Circumferential stress of the V-band clamp at different locations around V-band clamp, C is constant, (b) Comparison with theoretical analysis, μ=0.15, ϕ=20 °.

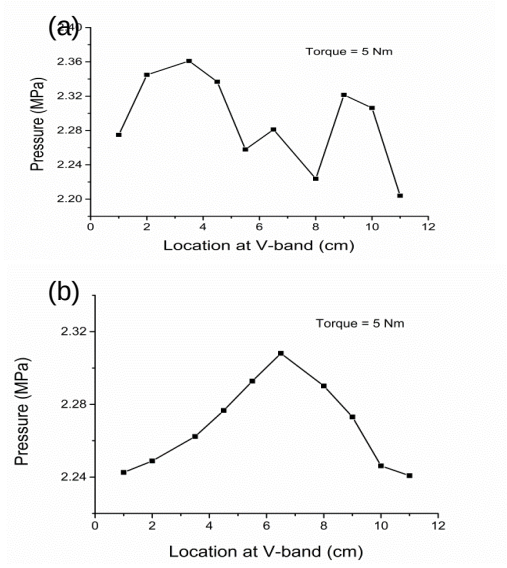

Fig 4. Contact pressure (a) Around upper piece of V-retainer (location is the distance away from the top of clamp), (b) Around bottom piece of V-retainer

In order to measure the load pressure, the sensor is placed between V-retainer and manifold, or between V-band clamp and bellow. The locations of sensors around V-retainer are illustrated in Fig. 1(a). The results show uneven distribution of contact pressure along V-retainer (Fig. 4). The maximum torque 5Nm is applied since higher torque will break sensor and fail to output reliable data. T-Bolt bends obviously after applying half of the expected torque with good lubrication (Fig. 5(a)). In order to figure out the deformation situation of T-bolt on V-band clamp, three same strain gages were mounted on the surface of the T-bolt at the same cross-section circle with 120 degree apart on each one as Fig. 5(b) shows (S1A, S1B, and S1C are the three same strain gages).

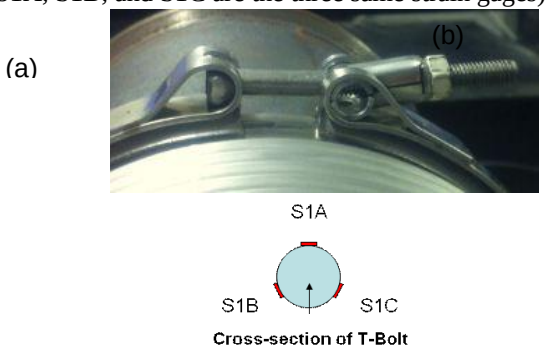

Fig 5. (a) Bend of T-bolt under service torque with lubricant (b) Strain gages installation on T-bolt

The strain of three strain gages is measured under different torques with the application of P-80 lubricant in Fig. 6. The results in Fig. 5(a) show the deformation direction of T-bolt is not along the axis, and it has some bend deformation upward. That means the yield stress of T-bolt that currently used on V-band clamp for full marmon is not enough and higher yield stress materials maybe a good option to make T-bolt. The negative strain at location S1A verified the compression at the top point due to the bend of T-bolt.

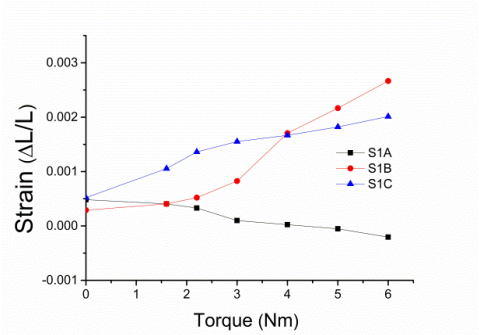

Fig 6. Strain gage sensors measurement under different torques.

III. FINITE ELEMENT MODELING AND SIMULATION

A scale 3D model including clamp, manifold and bellow used in the exhaust system is studied in this paper. The area of bellow sealed manifold clamped by the V-band is treated as rigid bodies because of its little deformation and heavy mass in comparison with that of the V-band clamp. The V-band clamp assembly is composed of a band, three pieces of V-shape retainers, T-bolt, trunnion and nut. The ends of the band are back bent to provide the pivoting holes for T-bolt and Trunnion. The band is reinforced with the V-shape retainers, onto which the retainers are resistance spot welded. The central angle of the arc of the V-shape retainer is 40 degrees. The inner surface radius of V-shape retainer is 79.10mm. The yield stress of clamp, manifold and bellow are

ISSN: 2277-3754
ISO 9001:2008 Certified
International Journal of Engineering and Innovative Technology (IJEIT)
Volume 4, Issue 3, September 2014

931, 380 and 172 MPa, respectively and Young's modulus is 200GPa and Poisson's ratio is 0.33. The lubricated friction coefficient of the contact pair of V-shape retainer against the manifold and bellow is 0.15. In this model, 41821 tetrahedral elements and 25184 triangular elements are meshed onto the entire clamp and local piping systems, as shown in Fig.7.

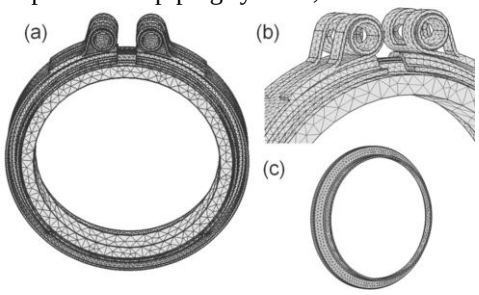

Fig 7. (a) Assembled clamp and piping system (b) Trunnion and back bend (c) Bellow

The contact properties between the manifold, bellow and clamp are specified using contact normal penalty factor. Friction effect is present in the three contact pairs. Bilinear model, based on the elastic and plastic properties, is used to describe the deformation of clamp. Spring foundation was constructed in FEA model to compliment the clamp deformation under interference fit assembly. A weak spring was added to the two domains and then specified the stiffness $k_x = k(1-p)2^{-(p.10)}$ of the spring as a function of parameter *p*. A value for the parameter k must be chosen so that the generated extra force balances the external load at the beginning. The stiffness of the weak spring should be ramped from a high value to 0 when the load was ramped to expected value. Given the initial model in Pro/E is of interference fit, simulations are accomplished twice with different constraints and loads. Because of the interference fit model of FEM, further approach of the two ends of clamp under expected load is infeasible. A small load is tried to find the initial contact points as shown in Fig4. The corresponding stress and pressure are also less in the order of magnitude than the experiment test results. The stress caused by the misalignment of the center lines of the manifold inner and bellow is ignored during this analysis.

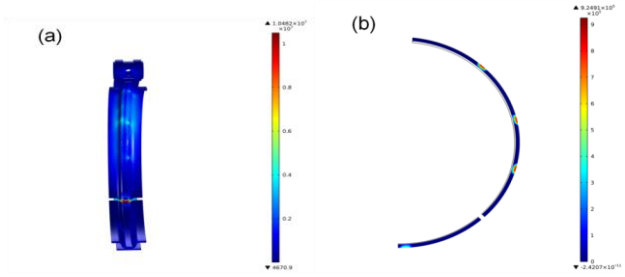

Fig 8. (a) von Mises stress distribution of clamp (b) Contact pressure distribution around bellow

Fig. 8 displayed the von Mises stress (Pa) of clamp and contact pressure (Pa) between V-retainer and bellow. In the FEA simulation results, the brighter the color of figures, the higher the stresses. Model is halved in this stage to simple the burden of calculation due to the symmetry of clamp. The maximum stress of clamp shows in gap between V- retainers. Under such lower load, the leap of stress can attribute to the reduction of cross section area. The contact pressure distribution in Fig.8 (b) tallied with the experiment test results in Fig. 4 which presented the contact pressure in the initial stage of loading. Those high pressure locations are initial contact points when load was ramping up. However, the real working torque is in the range of 12-15Nm torque to keep a certain pressure between components. Further experiment test is limited because piezoelectric sensor will be penetrated under high stress. Thus, another approached is carried out to simulate the contact pressure under working load. Similarly, a tension spring of stiffness k is applied between the pivots to stand for the required torque, which keeps the V-clamp in perfect contact with piping systems given the interference fit initial model. The equivalent stiffness, k, can be estimated because the specified torque on the T-bolt for clamping can be converted to its clamping force in terms of torque-friction coefficient, nominal bolt diameter and thread angle, with its displacement. Since the conversion from torque to clamping force is empirical, often significant variations can be observed. Thus the spring forces can be expressed with the stiffness, k with a specified range. In the simulations of this research, the stiffness, k, ranges from 1×10^6 to 1×10^7 N/m, to reflect various torques on the T-bolt and nut, also for studying its variations. k = 1×10^6 N/m, is chosen as demonstration in Fig. 9.

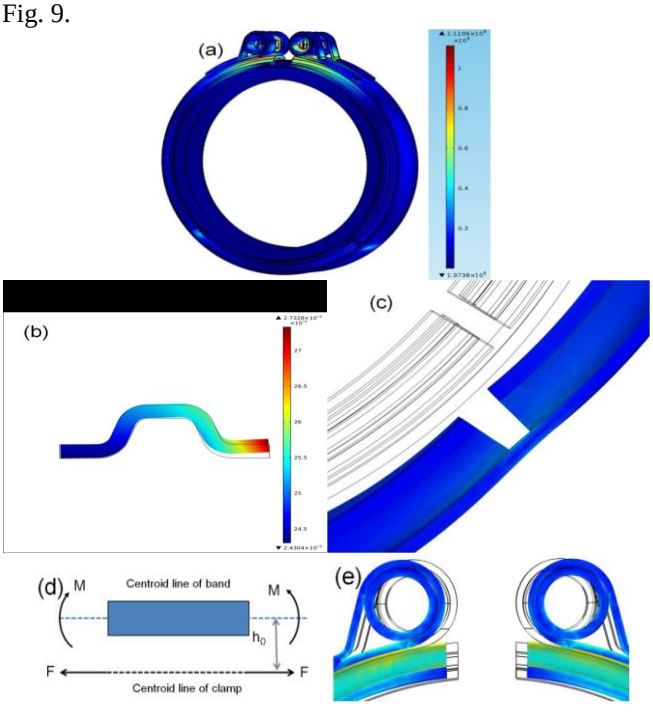

Fig 9. (a) Von Mises stress (Pa) distribution of model; (b) Displacement (m) of V-shape band (scale factor=15); (c) Deformation of gaps at the bottom side (scale factor 15); (d) Extra bending moment of band at gaps (The distance h_1 = 3.55 mm); (e) Displacement of clamp after interference fit relaxed.

For given spring forces, their effects on the stress distribution are studied. The tension induced by the spring

ISSN: 2277-3754
ISO 9001:2008 Certified
International Journal of Engineering and Innovative Technology (IJEIT)
Volume 4, Issue 3, September 2014

produces the circumferential force and wedging force for the pipe joint systems. Based on the geometry of the clamp and piping systems, it is reasonable to assume from Fig. 9(a) that the deformation occurs on the clamp, not on the piping systems, and the interference fits is relaxed. Fig. 9(b) demonstrates the V-retainer deformation in which the V-shape retainer opens up a little bit to keep the new equilibrium after the interference fits relaxed. The original profile of the V-shape retainer shown in black line and its deformed profile shown in color are compared. Under this circumstance, the surface-to-surface contact between the clamp and the piping systems are converted to line-to-surface contact with the opening up of V-band retainer. This numerical simulation indicated major relaxation or deformation is undertaken by one side of the V-retainer which is in touch with the much thinner bellow. Deformation of band at the bottom gaps are shown in Fig. 9(c) and the high stress can attribute to the less cross section area at the gaps between the V-retainers, and the extra bending effect. Table 2. lists cross section area, moment inertia and position of centroid line of the clamp, V-retainer and band. Since the two gaps are far away from the loading points, it is reasonable to assume that the circumferential force is in line with centroid line of clamp near the gaps. In Fig. 9(d), the distance h_1 from the centroid line of the band to the clamping force parallel to the centroid line can be geometrically determined. At the gaps, the bending stress caused by the offset of centroid lines superposing to the circumferential stress in the band results in a high von Mises stress.

Table 2. Cross section area, moment inertia, and position of centroid line away from the surface of band

Part	Area(mm^2)	Inertia(mm^4)	Centroid(mm)
Clamp	88.97	888.32	4.35
V-retain	58.41	352.83	5.97
Band	31.28	6.67	0.8

The stress concentrations and displacements near the clamp ends can be observed in Fig. 9(e). The higher the stress is, the smaller the displacement is. This is an important indication for the V-band clamp sealing. It is observed that there is a deformed profile shown in color in comparison with the original profile of the clamp, which is the displacement of the clamp after the relaxation from the interference.

Fig.10 (a) displays the COMSOL simulated contact pressure between clamp and bellow after the interference fit relaxations. The simulation results are extracted around the clamp from bottom to top and plotted in Fig.10 (b). The tendency of stress distribution tallies with the exponential distribution of the contact pressure, which is expressed in Table 1. In Fig.10 (a), the relatively high contact pressure between the manifold and bellow is observed in the area corresponding to the V-retainer gap on the clamp, and this is caused by the bending stress of the band. Under the trunnion of the clamp, there is the highest contact pressure between the manifold and bellow. Correspondingly, the band under the trunnion has higher yielding stress. Dekker[9] suggested that a slight vertical displacement of the bolting lug may help avoiding the yielding of clamp. The local high clamping force produces the decrease of the clamp curvature under the trunnion and the increment of the clamp curvature nearby, which causes a weak sealing to the piping system. Fig.10(c) shows the warping of clamp after relaxation of interference fit.

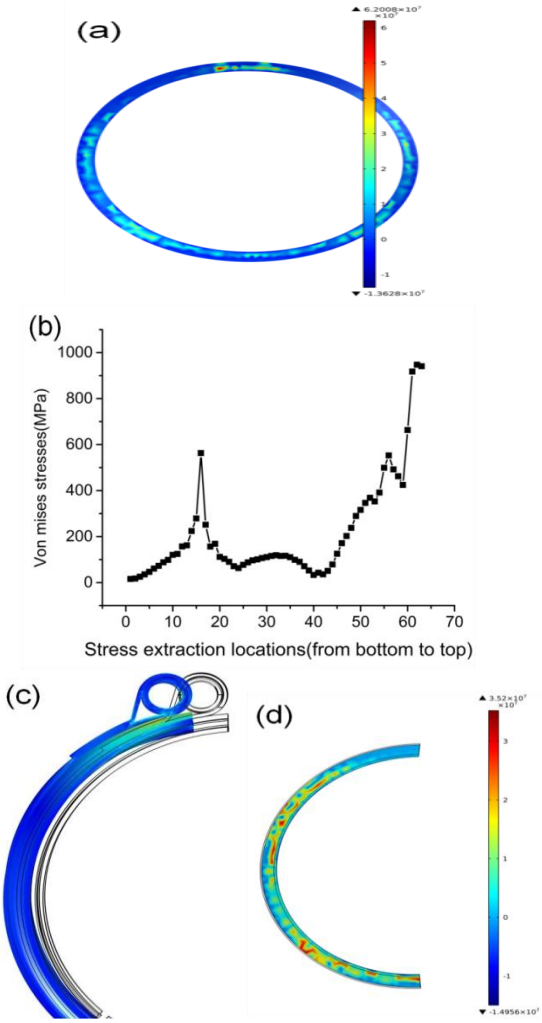

Fig 10. (a) Contact pressure distribution around bellow, (b) Distribution fitting around the clamp, (c) Warping of clamp, (d) Contact pressure with load applied along the centroid line of V-retainer

Per Saint-Venant's Principle, the radial force locally affects the stress distribution. Since the diametrical location of the V-band clamp centroid and the loading device are not the same, there will be local radial forces adjacent to the T-bolt and trunnion to transition the bolt force to the clamp centerline [1]. Therefore, higher stress appears beneath T-bolts due to the non-uniform radius load. Conforming and non-conforming contact are employed to describe the stress distribution beneath the trunnions [10]. Considering the

ISSN: 2277-3754
ISO 9001:2008 Certified
International Journal of Engineering and Innovative Technology (IJEIT)
Volume 4, Issue 3, September 2014

relative positions of trunnion and clamp, when the non-conforming contact distribution is assumed, the analytical results indicate that the corresponding length of contact area is only 0.2mm when the T-bolt is fastened to the specified torque. However, the COMSOL simulated high contact pressure area is much larger than that of the non-conforming contact analysis. If the conforming contact distribution between the clamp and the piping systems is assumed, the load transferred from trunnion can be regarded as point load. The conforming contact without interfacial friction is analyzed to evaluate the stress distribution. When the clamp and the piping systems are finishing fastening together, the contact area grows rapidly along with loading until it takes up a considerable portion of the contacting bodies. The analytical solution has been proposed by Noble [11] using stress function method based on a loaded pin in a hole in a plate model. Similarly, Man [12] obtained contact stress distribution of perfect fit loaded pin in a hole in a plate using boundary element method. The result from Man [12] tallied with the analytical solution of Noble [11]. Shtaerman [13] produced an expression about the pressure distribution $P_n(x)$ in the case of two dimensional contact as:

$$P_n(x) = nA_nE^*a^{2n-2}\{(\frac{x}{a})^{2n-2} + \frac{1}{2}(\frac{x}{a})^{2n-4} + \ldots + \frac{1.3\cdots(2n-3)}{2.4\cdots(2n-2)}\}(a^2-x^2)^{1/2} \quad (1)$$

Where a is radius of inclusion or contact arc. In this equation, initial separation of two contact surfaces is represented using a polynomial. n and An are the degree of approximation and coefficient of degree separately. Those researches about conforming contact indicated a relative higher maximum stress when the contact arc is short, and vice versa. In comparison with the COMSOL simulation results shown in Fig.10, it is concluded that, due to the complicated structure of the V-band clamp, the real stress distribution can be more precisely described by combining the effect of conforming and non-conforming contacts. For the non-conforming bodies, of either identical or incompressible materials (Poisson ratio is 0.5), the frictional traction can be regarded as absent and then Hertz contact solution is applicable. Actually, even to the bodies of the dissimilar materials, the non-conforming contact with friction can increase no more than 5% of the total load required to keep a contact area predicted by the Hertz theory[14]. In another word, friction traction effect is negligible when contact stress distribution of the point load is considered. Fig.10 (d) shows the contact pressure distribution when load is applied along the centroid line of V- retainer. This comparative simulation is carried out assuming that the loading area is in line with the centroid line of V-retainer segment, as shown in Fig.11 (b). The control test is applied to verify the influence of moment of the stress distribution. The moment arm h_3 = 1.76mm leads to upward bending moment. In the far away region of the loading area, manifold and bellow are still in good connection. Since the upward bending moment greatly weakens the wedge effect, thus the force in normal direction is less transformed to the contact plane of the manifold and bellow. As a result, the lowest stress area appears immediately in the loading zone and that verifies the case as shown in Fig. 10(d). The bending moment of the clamp showed in Fig. 7(a) is caused by the offset between the centroid line of the clamp and the direction of tension force F produced by the bolt torque. The moment arm of F is the superposition of h_1 = 4.17mm and h_2 = 0.8mm.

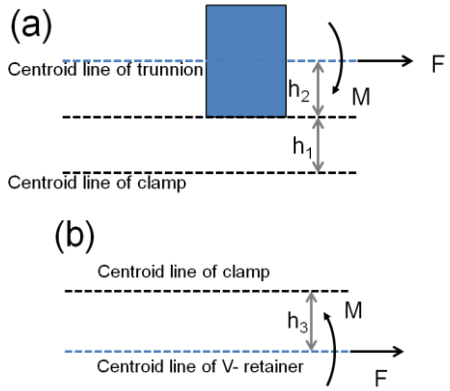

Fig 11. (a) Centroid line and load on trunnion, (b) Centroid line and load on V-retainer

It is also possible to eliminate the peak stress and avoid the nearby warping effect through changing the design of T-bolt. Bolt torque and bolt clamping force between the bolt and clamped parts is assumed as linear relationship. Because it is observed that the T-bolt is often slightly bent downwards, load transferred to clamp will be reduced, which implies that the specified torque failed to reach the desired connecting effect. Furthermore, the offset will lead to a more serious deterioration of the contact pressure distribution because vertical component of load leads to a downward bending moment again, and it causes the clamp band warping. Inspired by this fact, if the bolt is designed with a pre-bent bolt stem, whose bending is opposite to the downward bending, a bending moment produced by a component of the clamping force can help balance the initial bending moment caused by offset of centroid line. As a result, the reaction force is much smaller than that of the original design, thus the warping effect will disappear. These results illustrated that a reduced reaction force distribution beneath the loading area resulted from a reasonable pre-bent bolt design is able to cancel the offset of bending moment. A properly designed pre-bending angle of the bolt would be able to guarantee that all contact pressure can reach the desired wedging values, and improve the consistency as well as the reliability of assembly. Besides, special material treatment may be needed to maintain strength and shape after the pre-bending deformation of the bolt. The back bend is hold on to the band by resistive spot welding and the location of the first spot location also has the effect of reducing the peak stress and preventing the warping of the band. Tangential backbend is also suggested since the design could lengthen the reaction area and then reduce the peak pressure effect.

ISSN: 2277-3754
ISO 9001:2008 Certified
International Journal of Engineering and Innovative Technology (IJEIT)
Volume 4, Issue 3, September 2014

IV. CONCLUSION

In this paper, an interference fit model between the V-band clamp and the piping systems is thoroughly analyzed through FEA, experiment test and theoretical modeling. The circumferential strains measured by piezoelectric sensors are tallies with the exponentially decreasing pattern from the top to the bottom of the V-band clamp. Contact pressures under the low load from FEA simulation match well with experiment test to find the initial contact points. FEA results under service load demonstrate that there are abnormal high contact pressures beneath trunnions, and extremely low pressures at the end of the back bend because of the clamp warping. Point load and contact mechanics are employed to explain the contact pressure deviation from the classical theory. Offset between centroid line of clamp and direction of tension force causes bending stress and attributes to the abnormal stress distribution. A pre-bent T-bolt design is suggested to counteract the effect of the offset.

REFERENCES

[1] "Marman clamp system design guidelines", Guideline GD-ED-2214, NASA Goddard Space F light Centre, 2000.

[2] K. Shoghi, S. Barrans, & H. Rao, "Stress in V-section band clamps," IMechE, vol.218, no.3, pp.251-261, March. 2004.

[3] G. L. Jones, "Evaluation of clamp effects on LMFBR piping systems," Swanson Engineering Associates Corp., McMurray, PA (USA), Aug.1980.

[4] B. Parsons & E. Wilson, "A method for determining the surface contact stresses resulting from interference fits," J MANUF SCI E, vol.92, no.1, pp.208-218, Feb.1970.

[5] J. Mucha, "Finite element modeling and simulating of thermo-mechanic stress in thermo-compression bondings," Mater. Des, vol.30, no.4, pp.1174-1182, April 2009.

[6] Y. Zhang, B. McClain, & X. Fang, "Design of interference fits via finite element method," IJMS, vol.42, no.9, pp.1835-1850, Sep.2000.

[7] J. Oda, J. Sakamoto, & K. San, "A method for producing a uniform contact stress distribution in composite bodies with interference," STRUCT OPTIMIZATION, vol.3, no.1, pp.23-28,1991.

[8] Z. Qin, S. Yan, & F. Chu, "Finite element analysis of the clamp band joint", APPL MATH MODEL, vol.36, no.1, pp.463-477, Jan. 2012.

[9] C. J. Dekker & W. J. Stikvoort, "Improved design rules for pipe clamp connectors," INT J PRES VES PIP, vol.81, no.2, pp.141-157, Feb. 2004.

[10] K. L. Johnson & K. K. L. Johnson, "Contact mechanics," Cambridge university press, 1987.

[11] B. Noble & M. Hussain, "Exact solution of certain dual series for indentation and inclusion problems," INT J ENG SCI, vol.7, no.11, pp.1149-1161, Jan. 1969.

[12] K. Man, "Contact mechanics using boundary elements," 1994.

[13] I. Y. Shtaerman, "To Hertz's theory of local deformations in compressed elastic bodies," In CR (Dokl.) Acad. Sci. URSS, vol.25, no.5, pp.359-361. 1939.

[14] D. Spence, "The Hertz contact problem with finite friction," J ELASTICITY, vol.5,no.3-4, pp.297-319, Nov.1975.

AUHTOR'S PROFILE

First Author Ph.D. student at mechanical engineering Technology of Purdue University, West Lafayette, IN, US.

Second Author Post-Doctoral at mechanical engineering Technology of Purdue University, West Lafayette, IN, US.

Third Author Prof. at mechanical engineering Technology of Purdue University, West Lafayette, IN, US.